Dataset Augmentation Allows Deep Learning-Based Virtual Screening To Better Generalise To Unseen Target Classes, And Highlight Important Binding Interactions

Jack Scantlebury,[*,†] Nathan Brown,[*,‡] Frank Von Delft,[*,¶,§,‖] and Charlotte M. Deane[*,†]

†*Department of Statistics, University of Oxford, 24-29 St Giles, Oxford, OX1 3LB, UK*

‡*BenevolentAI, 4-8 Maple St, London, W1T 5HD, UK*

¶*Structural Genomics Consortium (SGC), University of Oxford, Oxford, OX3 7DQ, UK*

§*Diamond Light Source, Harwell Science and Innovation Campus, Didcot OX11 0DE, UK*

‖*Department of Biochemistry, University of Johannesburg, Aukland Park, Johannesburg 2006, South Africa*

E-mail: jack.scantlebury@hertford.ox.ac.uk; nathan.brown@benevolent.ai; frank.vondelft@sgc.ox.ac.uk; deane@stats.ox.ac.uk

Abstract

Current deep learning methods for structure-based virtual screening take the structures of both the protein and the ligand as input but make little or no use of the protein structure when predicting ligand binding. Here we show how a relatively simple method of dataset augmentation forces such deep learning methods to take into account information from the protein. Models trained in this way are more generalisable (make better predictions on protein-ligand complexes from a different distribution

to the training data). They also assign more meaningful importance to the protein and ligand atoms involved in binding. Overall, our results show that dataset augmentation can help deep learning based virtual screening to learn physical interactions rather than dataset biases.

Introduction

A series of recent papers has shown that some deep learning methods designed for structure-based virtual screening can accurately separate actives and decoys when given only the structure of the ligand.[1–3] These results indicate that such methods are learning differences between the properties of actives and decoys, rather than the physical interactions between the receptor and the ligand. From this it is possible to conclude both that the methods will fail to generalize well (predict on datasets far removed from the training data), and that there are significant flaws in the current training datasets and/or regimens.

The task of a virtual screening algorithm is to distinguish between bound structures where the small molecule is an active, and those where it is a decoy. A standard structure-based virtual screening technique docks potential drug-like compounds into a protein target of interest, and ranks them according to a physically-inspired scoring function (for a review of common virtual screening techniques including docking, see [4]). These methods can be used to screen vast numbers of potential compounds for target interactions and are extremely cheap compared to lab-based experiments.[5] The accuracy of docking, however, is highly target-dependent.[6] This issue, along with the current deluge of structural data, has prompted the use of machine learning methods in structure-based virtual screening and in the verification of docked structures.[7–9]

Machine learning has found its way into many scientific domains, and drug discovery is no exception (a review can be found in [10]). Multiple machine learning-based virtual

screening methods have been developed. Most of these rely on 1- or 2-D descriptors - that is, they take as input a representation of the ligand as a fingerprint,[11] graph[12,13] or other descriptors,[14] and the protein (if present at all) as a sequence of amino acids.[13] More recently, machine learning methods which are able to capture specific spatial and chemical interactions between the protein and ligand have been introduced; the major driver for building these more complex methods is the hope that because they can learn physicochemical interactions between protein and ligand, they should be able to more accurately predict the binding of ligands and proteins far removed from the complexes on which they were trained (be more generalisable). The current state-of-the-art method for attempting to capture these types of spatial interactions is the convolutional neural network (CNN).[15]

CNNs are a type of deep neural network which, due to their ability to capture spatial relationships between objects, are commonly used in image classification. The gnina framework for virtual screening[16] treats docked structures as 3D images with different channels for different types of atoms as inputs into a CNN and outputs a binary classification (active/decoy). A CNN with three hidden layers built in the gnina framework and trained and tested on part of the DUD-E dataset[17] was shown to perform better in the task of virtual screening than using the docking score of AutoDock Vina. It had a mean test target ROC-AUC of 0.862, compared to 0.703 for AutoDock Vina (reported in [18]); a ROC-AUC score is the area under the curve of the receiver-operator characteristic graph, which is a measure of the ability of a classifier to correctly rank unseen labelled data. The same input format with a deeper and more densely connected network along with protein family-specific finetuning was used to develop the DenseFS CNN, which significantly increased predictive power to a mean DUD-E target ROC-AUC of 0.917.[18] This featurization method has also been used to explore the nature and role of hydration in protein-ligand binding.[19]

These results suggest that deep learning offers real potential in terms of structure-based

virtual screening. However, both CNN methods performed far worse on validation sets taken from a different database of structures (they generalize poorly). For example in the case of DenseFS, models trained on the DUD-E dataset and tested on an external dataset constructed from the ChEMBL database[20] performed significantly worse by every metric (mean test target ROC-AUC and mean precision) than when the same models were tested on DUD-E.[18]

It has been demonstrated many times that a machine learning model with good performance on held-out test data from the same distribution as the training data does not guarantee good performance on other data sets.[1,2,18] This lack of generalisability means that models cannot accurately classify ligands which are significantly larger or smaller than the molecules they were trained on, or ligands which are chemically distinct from the training data.

If the aim of generalisability to targets far from the training set is to be realized, it is important that structure-based virtual screening learn physical interactions between the protein and the ligand, rather than properties of the ligand. One way to identify if methods are learning such interactions is to visualize the importance of atoms or groups of atoms to the score. Hochuli *et al.* used several techniques to visualize which atoms and residues in the input to the original gnina network were important to the classification decision.[21] One method used was input masking, where the CNN is used to score the docked complex both with and without certain atoms or groups of atoms present. These scores can then be compared in order to ascertain the importance of these atoms or groups of atoms.

There have also been attempts to quantify what precisely is being learned by CNNs for virtual screening. It was recently shown that model performance for some methods does not suffer significantly when ligand structures in the test set are given without the protein

target/receptor.[2,3] The overall conclusion from these studies was that the methods are using very little if any information from the protein target. This finding links to the fact that in many of these datatsets, receptor-free methods such as k-nearest neighbours on ligand fingerprints perform almost as well as methods making use of the receptor.[1] It has even been shown that using a small number of simple 1D properties of ligand molecules is enough to classify accurately on the widely-used DUD-E dataset. The 50 decoys per active in the DUD-E dataset were chosen to have the same or similar values as the active molecule for six key properties (molecular weight, ClogP, number of hydrogen bond acceptors and donors, net charge and number of rotatable bonds) whilst remaining topologically distinct; classifiers trained using just these six supposedly unbiased properties achieved good performance on held-out DUD-E targets.[2] This result indicates that differences between the properties of actives and decoys in the DUD-E dataset without any protein information can be used for classification.

The high performance of CNNs for virtual screening when only given the ligand structure and the known biases in the dataset suggests that networks are not learning the physico-chemical interactions between the protein and the ligand, but are separating actives from decoys based on properties of the ligand alone.

A recent attempt to remedy this problem was made using both Maxiumum Unbiased Validation (MUV) and Asymmetric Validation Embedding (AVE). MUV is a measure of how clustered actives are and AVE measures how tightly clustered decoys are relative to the active-decoy distance. In [22], the distance between molecules was defined using their 2048-bit ECFP6 fingerprint, and 'unbiased' training sets were generated by minimising either MUV or AVE with a genetic algorithm. The training data was 189 targets each with at least 500 actives. Two types of tests sets were generated: 'standard-AUC' sets consisting of randomly selected (non-training) ligands, and 'far-AUC' sets which consist of ligands

that are considered to be far (Jaccard dissimilarity between ECFP6 fingerprints ≥ 0.4) from ligands in the training set for that target. It was found that the original ('biased') models which performed well on standard-AUC often failed to perform as well on far-AUC, showing the expected lack of generalisability. However, training on the unbiased training sets led to a drop in performance on far-AUC, meaning that this type of debiasing is ineffective for improving generalisability.

In this paper, we test how CNNs use receptor information and explore methods to improve their generalisability. First, we compare the behaviour of deeper CNNs to their shallower counterparts, and find that deeper CNNs use more information from the receptor, but their classifications are still heavily reliant on the identity of the ligand. Given this result, we develop a procedure to force the CNN to learn from the protein/ligand interactions. We augment the training dataset with active ligands incorrectly positioned and labelled as decoys. In order to analyse the effect of this augmentation, we look both at the ability of the method to predict and the distribution of CNN scores attained for different training conditions. On cross-validation (training and testing on different parts of the DUD-E dataset), there is no significant difference in performance between the original and new methods, but the score distributions show increased sensitivity to receptor information when training data is augmented in this way. Finally, to demonstrate the method trained with this augmented dataset is learning physical interactions, we show both that the method is more generalisable, it performs significantly better on an external test set, and that atoms involved in interactions between the ligand and receptor are now important to the score.

Methods

To probe what is being learned by CNNs for virtual screening and to develop methods to force the learning of physical interactions, three facets of the problem were explored. These

were: the network architecture (model), the training set, and the presence or otherwise of receptor information in the test sets.

Datasets

All training was carried out using the Database of Useful Decoys - Extended (DUD-E).[17] To carry out initial tests, a three-fold cross validation strategy on DUD-E was used. External validation was carried out using the same subset of targets and ligands from the ChEMBL dataset[20] as in the previous study of Imrie *et al.*[18]

DUD-E

The Database of Useful Decoys Extended (DUD-E)[17] is comprised of more than 22,000 actives and 1,100,000 decoys across 102 protein targets. Actives are molecules which have been experimentally determined to bind in the binding pocket of a protein target, and for each active, there are 50 decoys which are assumed to be non-binders. All actives and decoys are docked into the binding site using AutoDock Vina.[23] The decoys in DUD-E were generated to have similar physicochemical properties to their active (molecular weight, log-P, number of hydrogen bond acceptors and donors, net charge and number of rotatable bonds), but were designed to be topologically distinct.

Following the methodology of Imrie *et al.*,[18] three folds were constructed from DUD-E where protein targets with $\geq 80\%$ sequence identity were placed in the same fold, to avoid training on structures that are similar to those in the test fold. The details of these folds can be found in the supplementary information (Table S1). Intra-dataset validation was carried out by training on two folds with the remaining one used for testing, giving three possible permutations.

Each DUD-E target can also be categorized into one of the following families, with

numbers indicating the number of targets per category: Kinase (26), Protease (15), Nuclear (11), G protein-coupled receptor (GPCR) (15) and Other (45).

ChEMBL

A set of 50 ChEMBL targets determined to be a suitable benchmark set for 2D fingerprinting methods was compiled by Heikamp and Bajorath.[24] Of these, a subset of 14 targets which had $\leq 80\%$ sequence similarity to all DUD-E targets were chosen as an external validation set in both Ragoza *et al.*[16] and Imrie *et al.*.[18] There are nine docked structures for each active, all of which are labelled as active. For each active ligand, there are $\sim$100 decoy ligands, again each with nine docked structures labelled as decoys. This gives 12,275 active structures over 14 targets, with 1,363 unique active ligand molecules, along with 1,238,178 decoy structures.

CNN Architectures

Gnina[16] defines the binding site as a cube with sides of 24 Å centred on the ligand, which it splits into $48 \times 48 \times 48$ voxels, each with sides of length 0.5 Å. It also constructs 34 channels, each containing the pseudo-electron density from a different atom type, and designated as either a 'ligand channel' (18) or 'protein channel' (16). The density at each voxel is calculated using a piecewise combination of a Gaussian and a quadratic function, both depending on the distance from the nucleus and the van der Waals radius. The combination of all 34 channels over the three dimensions gives a $48 \times 48 \times 48 \times 34$ tensor description of the input space which is used as the feature vector for the CNN. The two models described below both use this featurization method, but differ in the network architecture used for classification. The authors of Gnina have released a standalone version of *libmolgrid*[25] (the featurization part of Gnina), which can be found at https://gnina.github.io/libmolgrid.

Gnina: A network with three convolutional layers (each followed by a max pool), then a

fully-connected final layer with a softmax activation function, giving a probability over the two categories (active/decoy). This version of the CNN[16] was the subject of all the analyses so far carried out into the importance of the receptor in active/decoy classification.[1–3]

DenseFS: A much deeper network with three sets of four densely connected convolutional layers followed by a fully-connected softmax layer and cross entropy loss.[18] This network significantly improved performance over the Gnina network on both held-out DUD-E targets and the ChEMBL set.

Training Schemes

Training was carried out using the original DUD-E dataset as well as three different augmented datasets:

- **DUD-E-Original**

  The original DUD-E dataset, using the docked poses provided in Ragoza *et al.*[16]

- **DUD-E-Trans**

  DUD-E-Original, augmented with three copies of each active, in a random conformation and translation. See Protocol 1 and Fig. S1 in the supplementary information for the full protocol and a visual example.

- **DUD-E-Redocked**

  DUD-E-Original, augmented by taking each active, and redocking it into the binding pocket with AutoDock Vina to generate up to 20 poses. The three highest ranked (lowest energy) poses at least 5Å root-mean-squared distance (RMSD) from the active pose were labelled as decoys and used in training.

- **DUD-E-Hybrid**

  Both augmentations from DUD-E-Trans and DUD-E-Redocked were added to the training set, giving a total of six extra decoys per active.

Models

From hereon in, **Baseline** will refer to models with the Gnina architecture trained on all or part of DUD-E-Original and **OriginalFS**, **TransFS**, **RedockedFS** and **HybridFS** to classifiers with the DenseFS architecture trained on all or part of DUD-E-Original, DUD-E-Trans, DUD-E-Redocked and DUD-E-Hybrid respectively.

Ligand-and-Receptor and Ligand-Only Tests

The two tests described in this section (Ligand-and-receptor and Ligand-only) were conducted according to the same protocol, the only difference being the presence or absence of the receptor in the test set structures. As described above and following Imrie *et al.*,[18] three folds were constructed from the 102 DUD-E targets (Table S1 in the supplementary information). A model was trained on two of the three folds, with the final one reserved for testing. Test predictions from all three models were concatenated for easier visualisation of results. This protocol is depicted in Fig. S2 in the supplementary information.

Models for the Ligand-and-receptor and Ligand-only tests

Three separate CNNs (one for each fold) were trained using each of the five CNN models described above, giving a total of 15 trained models. Training was conducted with a batch size of 16, for 25,000 iterations and the number of actives and decoys in each batch was even.[18] The optimizer used was stochastic gradient descent, with a base learning rate is 0.01, an inverse learning rate power decay value of 1, a gamma value of 0.001, a weight decay of 0.001, with a momentum of 0.9.

Ligand-and-receptor Test

Once the models were trained according to the above protocol, they were tested on each of the test folds with no changes. This was the Ligand-and-receptor test.

The Ligand-only Test

A receptor-free version of each test fold was generated. For every case (actives and decoys) the protein was removed from the structure file leaving only the docked ligand in the pose it has in the protein binding pocket. This was the Ligand-only test.

ChEMBL Validation

In order to investigate the effect of our training data augmentation on how CNNs generalize to data from a different distribution to the training set, three CNNs were trained on the entire DUD-E dataset (or an augmented version) with different random seeds. These CNNs were then used to classify actives and decoys in our ChEMBL validation set. Following Imrie *et al.*,[18] the score assigned to each structure was the mean of the three CNN scores; the score assigned to a ligand with a target was the mean of the scores given to the top five (of the nine) structures. This system is illustrated in the supplementary information (Fig. S3). All training was conducted with the same hyperparameters as outlined above.

In Imrie *et al.,*[18] models were first trained on DUD-E in the same way as described in the methods section. However, the authors also made use of 'finetuning', a process of further tweaking all or part of the network for specific tasks. In this instance, copies of the initially trained networks were trained on different families on DUD-E, and then the test data was filtered according to family and the network such that the network that would be used to classify would be that which was finetuned on the training data from that family. This was reported to greatly improve discriminative power. We did not to employ that method, as the aim is only to test if augmentation improves generalisability of the model.

Masking

Classifications from neural networks are notoriously difficult to interrogate. The masking method of Hochuli *et al.* attempts to obtain the contributions from different residues in the binding site, and different atoms of the ligand.[21] In short, a trained model is given a bound structure, and then the same structure with different ligand atoms or receptor residues removed (the structure is 'masked'). The difference in CNN score between the full structure and the masked structure is taken as the contribution of whichever entity was removed (see Fig. S5 in the supplementary information). This difference is then converted to a percentage of the original CNN score. The sum of all of the individual atomic contributions need not in general add to 100%, because the relationship between the input features and the CNN score is nonlinear.

In the original paper (and accompanying software), only residue contributions from the receptor were calculated. Here we modified the software to mask individual atoms of the protein, in order to gain a higher resolution image. The PDB[26] structures used for masking (10OH and 1W4O) and were chosen to be the same as those used for masking by Hochuli *et al.* in [21] for ease of comparison. Neither of the PDB structures contains protein/ligand combinations found in DUD-E.

Methods of Assessment

Two metrics were used to measure the discriminative power of the classifiers, the area under the curve for receiver-operator characteristic graph (ROC-AUC) and the area under the curve for the precision-recall curve (PR-AUC). While the ROC-AUC usually lies between 0.5 and 1.0 (for random and perfect classifiers), the PR-AUC will usually lie between $\frac{n_{actives}}{n_{total}}$ and 1.0, where $n_{actives}$ is the number of actives in the test set and n_{total} is the total test set size. These lower bounds (which represent the performance of a random classifier) are ~ 0.02 and ~ 0.01 for the DUD-E test sets and ChEMBL validation sets respectively.

The use of ROC-AUC as a metric for model performance on highly imbalanced datasets such as DUD-E (50:1 actives:decoys) or the ChEMBL set used here (100:1) has been shown to be less useful than PR-AUC.[27] ROC-AUC is widely reported for classification algorithms and is included here for ease of comparison with other work.

Results and Discussion

Only results using models trained on DUD-E-Original (OriginalFS) and DUD-E-Trans (TransFS) will be discussed here. The results for DenseFS architectures trained on DUD-E-Redocked (RedockedFS) and DUD-E-Hybrid (HybridFS) showed similar trends to TransFS, and are given in Table S3.

Ligand-Only Test

The precision-recall (PR, left) and receiver-operator characteristic curves (ROC, right) for the Ligand-and-receptor test (green) and Ligand-only test (purple) for the Baseline, OriginalFS or TransFS models are shown in Fig. 1.

Performance of Baseline. Fig. 1 (a, b) shows the PR and ROC curves for Baseline models tested both with and without the receptor present. The difference in the area under the ROC curves (ROC-AUC) between the Ligand-and-receptor and Ligand-only tests is just 0.031 (3.5%, 0.867 to 0.836). This agrees with the previous findings by Chen *et al.*[1] that performance is hardly affected by the removal of the receptor. The area under the PR curve (PR-AUC) drops by 0.061 (27.9%, 0.219 to 0.158) which is a larger change, but both metrics reflect that a large percentage of predictive ability is still retained in the Ligand-only test. This result indicates that the Baseline model is not relying significantly on information from the receptor channels for its classifications.

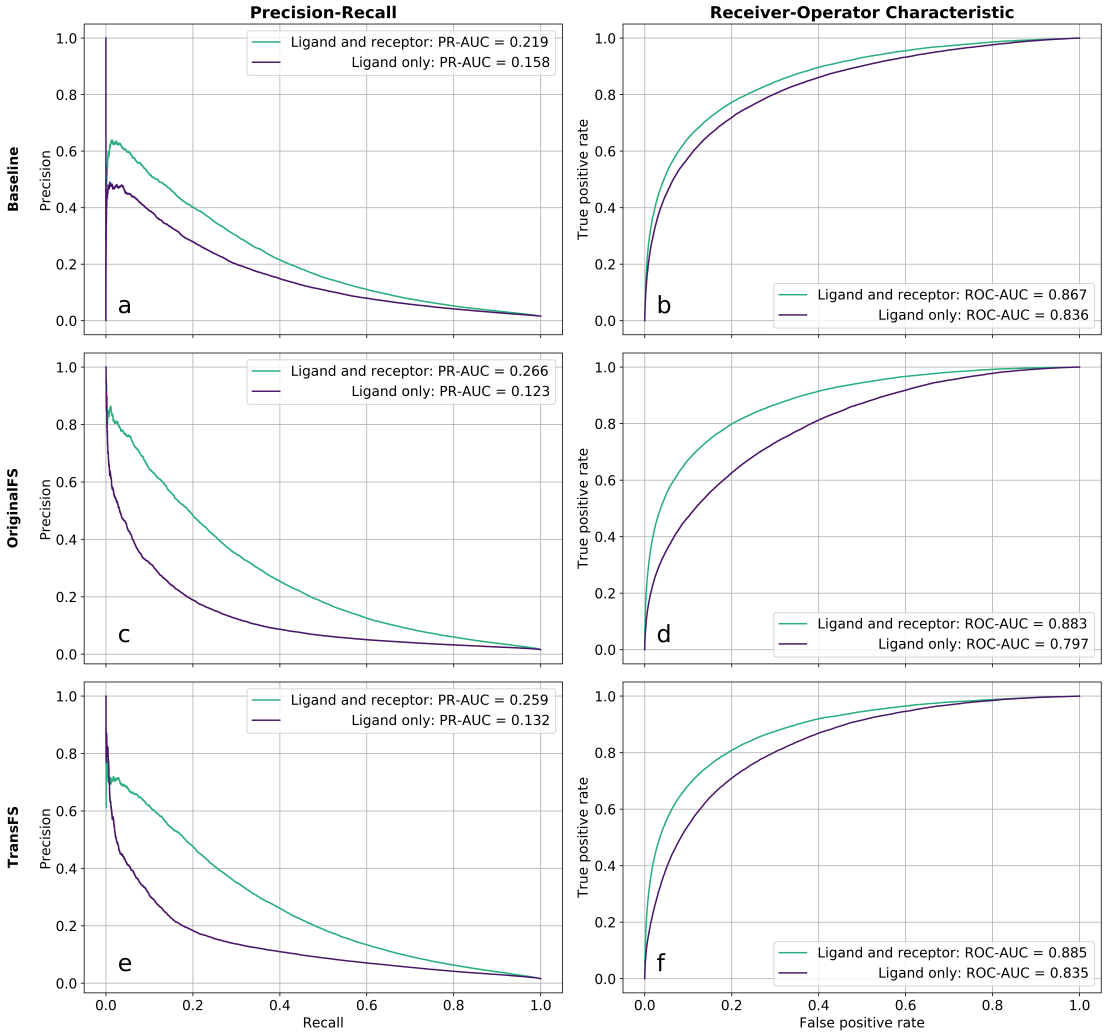

Figure 1: Removing receptor information does not cause total collapse in discriminative power for Gnina or DenseFS-based CNNs. Precision-recall and receiver-operator characteristic curves for the Ligand-and-receptor and Ligand-only tests. Models shown are Baseline (a, b), OriginalFS (c, d) and TransFS (e, f). Green lines indicate held-out DUD-E target test sets with both receptor and ligand information (Ligand-and-receptor test); purple lines are the same set but with only ligand information given (Ligand-only test).

Performance of OriginalFS. Fig. 1 (c, d) shows the PR and ROC curves for the Ligand-and-receptor and Ligand-only tests, using OriginalFS. The drop in performance when receptor information is removed is far larger than the drop seen for the Baseline. The ROC-AUC drops by 0.086 (9.7%, 0.883 to 0.797) and the PR-AUC decreases by 0.143 (53.8%, 0.266 to 0.123). The larger reduction in predictive ability when the receptor is not present indicates that the more expressive DenseFS CNN architecture uses receptor information more in its classifications than Gnina. However, there is still significant predictive ability in the ligand-only test. OriginalFS is still able to relatively accurately separate actives from decoys using only ligand information.

In an effort to force the DenseFS CNN to learn more from the receptor and how it interacts with the ligand, we trained TransFS using our augmented DUD-E set, DUD-E-Trans. The network therefore sees examples of active ligands in non-physical positions and conformations marked as decoys as well as the correct active poses.

Performance of TransFS. Fig. 1 (e, f) shows the PR and ROC curves for the Ligand-and-receptor and Ligand-only tests, using TransFS. The performance is very similar to OriginalFS; the difference in ROC-AUC is 0.050 (5.6%, 0.885 to 0.835) and PRC-AUC drops by 0.127 (49.0%, 0.259 to 0.132). This is surprising, as the TransFS models trained with DUD-E-Trans have seen examples of active ligands in non-physical structures labelled as decoys, which should remove the ability of the network to classify based on ligand fingerprint alone.

For OriginalFs and TransFS there is a significant but similar drop in performance when the receptor is removed. This suggests that using the DUD-E-Trans augmented training set is not causing greater use of the receptor in classification. In order to explore what, if any, influence training using DUD-E-Trans has, we examined the distributions of the raw CNN

scores.

The effects of training set on raw CNN scores for actives and decoys in the ligand-only test are shown in Fig. 2. The width of the plots of a particular CNN score is proportional to the relative density of structures assigned that score. Plots are split by training set, whether structures are actives or decoys, and whether a receptor was present (green) or not (purple) in the test set.

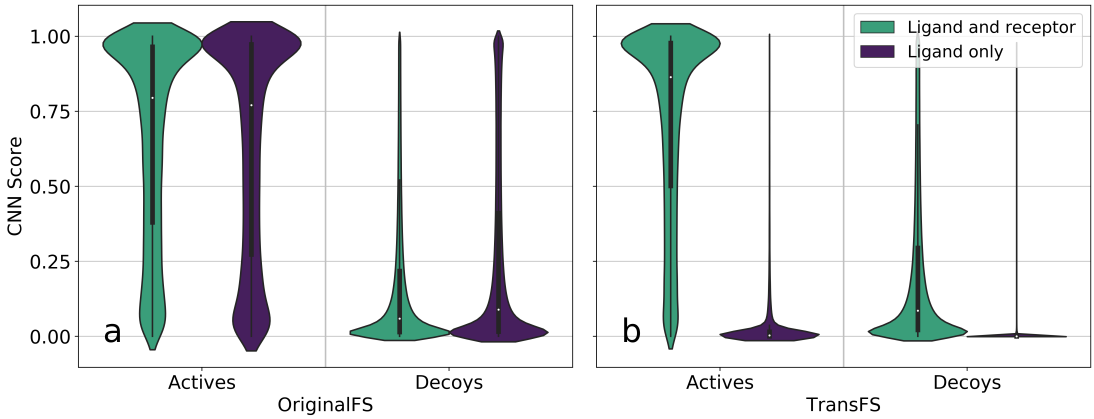

Figure 2: CNN score distributions reveal presence (OriginalFS) and absence (TransFS) of discriminative power when receptor information is removed in Ligand-and-receptor and Ligand-only tests. Violin plots of test set scores given to actives and decoys by OriginalFS and TransFS, with score distributions given with ligand and receptor information present shown in green and with ligand information only in purple. Plots *a* and *b* show distributions for OriginalFS and TransFS CNNs respectively.

Score distributions for OriginalFS. Fig. 2a shows the distributions of pose scores given to actives and decoys in the Ligand-and-receptor (green) and Ligand-only (purple) tests by OriginalFS CNNs. Neither actives nor decoys exhibit a significant difference in pose score distribution between the Ligand-and-receptor and Ligand-only tests, i.e. the green (Ligand-and-receptor) and purple (Ligand-only) plots for actives are almost identical. Compared to Baseline (Fig. S4a in the supplementary information), decoys in the Ligand-and-receptor test are skewed more towards zero, but actives in the Ligand-only test are in fact skewed

more towards higher scores, showing that using the deeper network alone does not guarantee the use of receptor information.

Score distributions for TransFS. Fig. 2b shows the same tests as Fig. 2a, using TransFS. Compared with OriginalFS (Fig. 2a), the score distributions for when the receptor and protein (Ligand-and-receptor) are present do not change significantly. However, the distributions for the Ligand-only tests collapse to being highly clustered near zero - for actives, the median score goes from 0.864 to 0.0292 when the receptor is removed, and for decoys the median drops from 0.0855 to 0.000132. These results show that receptor information is being used to generate a significant proportion of the score of the CNN for TransFS.

However, it is not evidence that it is being used in the way that we desire (to pick out physicochemical interactions). In order to test if receptor information is now being used in this way, we next test performance on an external validation set to test for generalisability. As described in the introduction, the ability to better classify structures from a different distribution to the training data would imply that general physical rules have been learned.

ChEMBL Validation

In order to examine how well the OriginalFS and TransFS CNNs generalize, they were used to predict on the ChEMBL validation set (see methods). The results for each target in the ChEMBL set are given in Table 1.

TransFS performs as well as or better than OriginalFS for 13 out of 14 targets, suggesting that augmentation causes models trained on one dataset to generalize better, and have increased predictive power on a different dataset. For ROC-AUCs, see Fig. S2 in the supplementary information.

Table 1: TransFS causes CNNs trained on the DUD-E dataset to generalise better to an external validation set than OriginalFS. PR-AUC values for the 14 targets in the ChEMBL validation set for OriginalFS and TransFS CNNs. Highest values in a row are highlighted in bold.

Chembl Target	Protein Family	Targets from family in DUD-E	OriginalFS	TransFS	% Increase
10752	Kinase	23	**0.289**	0.272	-5.8
12670	Kinase	23	0.363	**0.374**	3.0
20014	Kinase	23	0.573	**0.580**	1.2
10378	Protease	15	0.047	**0.052**	10.1
10498	Protease	15	0.056	**0.078**	39.3
11534	Protease	15	0.062	**0.095**	53.2
219	GPCR	5	0.116	**0.153**	31.9
11279	GPCR	5	**0.039**	**0.039**	0.0
11631	GPCR	5	0.245	**0.264**	7.8
12968	GPCR	5	0.009	**0.011**	22.2
18061	Other (Sodium channel protein type IX α-subunit)	2	**0.031**	**0.031**	0.0
28	Other (Thymidylate synthase)	1	0.286	**0.363**	26.9
276	Other (Phosphodiesterase 4A)	1	0.318	**0.415**	30.5
11359	Other (Phosphodiesterase 4A)	1	0.214	**0.270**	26.2

Training with DUD-E-Trans (TransFS) rather than DUD-E-Original (OriginalFS) tended to give larger improvements in PR-AUC scores for targets from families which do not feature heavily in the DUD-E set such as proteases (see methods for an overview and Table S1 in the supplementary information for a detailed breakdown of DUD-E target families). The largest performance increases were seen for proteins in the 'Other' category - containing targets in families such as 'Phosphodiesterase 4A' and 'Thymidylate synthase' - which do not feature at all in DUD-E. This larger difference in performance for the more distinct targets is to be expected, as ligands which are active for one member of a protein family are likely to be active for others, so learning the fingerprint profile of ligands likely to bind to one member of a family will help performance on external validation sets which contain that family. This can be seen here in the performance on kinase targets, which is extremely close between the two different training regimens. There are 26 kinase targets in the DUD-E training set, and although the ChEMBL set does not contain any identical targets, ligands which are actives for one kinase are much more likely to be active for another. In our case this means that OriginalFS performs comparably on kinases to TransFS, and in the case of the ChEMBL kinase target with ID 10752, OriginalFS has a PRC-AUC that is 0.017 (5.9%) larger than the PRC-AUC achieved by TransFS.

Being better able to generalize to an external validation set, especially on targets from families not in the training set, suggests that more general rules of physical interactions are being learned. In order to look for more direct evidence of this, we used input masking to find which areas of the ligand and protein each CNN assigned importance to when making a classification.

Masking

Masking can be used to identify which parts of the feature vector are important in the classification given by a CNN, by 'covering' parts of the input and comparing the score to the

'uncovered' original (see supplementary information, Fig. S5). Here, we have used it to check the contribution of each individual atom in both the ligand and receptor. A CNN which learns physical interactions should give high (positive) masking scores to atoms involved favourable interactions such as hydrogen bonding, and negative scores to atoms involved in unfavourable interactions such as steric clashes. Masking was performed as outlined in the methods on PDB structures 10OH and 1W4O, two of the structures used for masking in Hochuli *et al.*[21] (Fig. 3), neither of which are present in DUD-E.

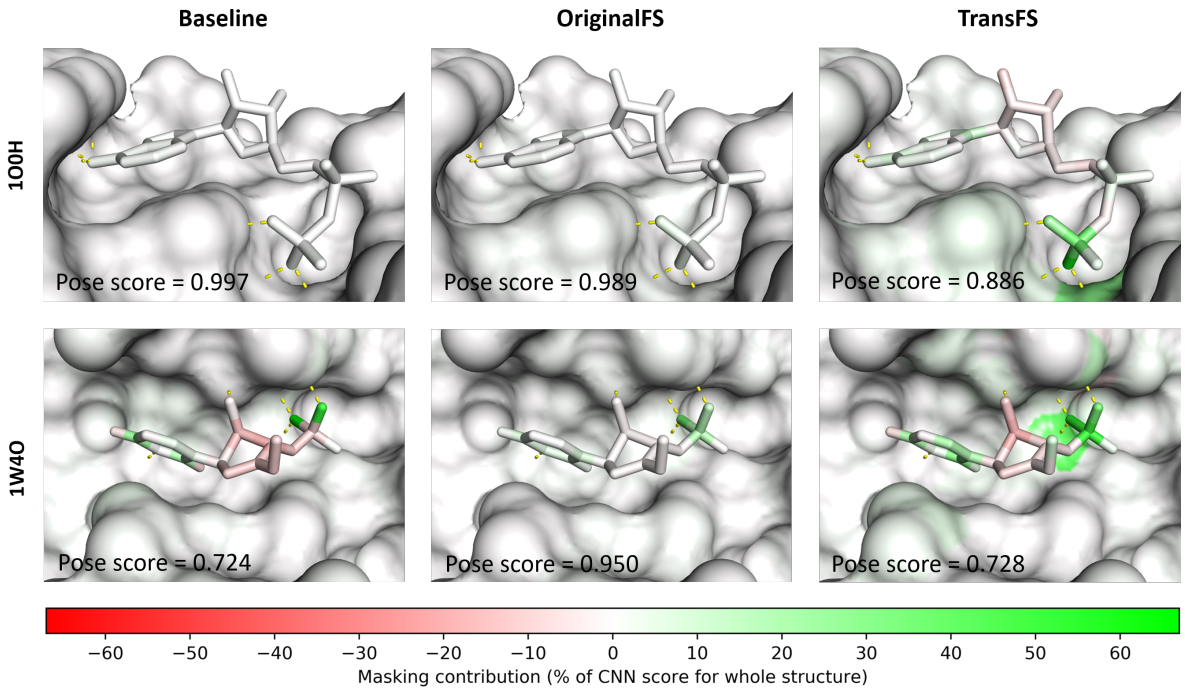

Figure 3: Masking using TransFS CNNs highlights important interactions between the ligand and protein. Results of masking for bound structures with PDB IDs 1O0H (top) and 1W4O (bottom). ned as donor/acceptor pairs within 3.5 Å of one another) are shown as yellow dashed lines. The pose scores from different networks and training sets are shown in the bottom left corners of each image. Color scale shows colors assigned for different masking scores, as a percentage of the pose score of the original unmasked structure.

Baseline (left). There is no contribution displayed by any of the atoms of the receptor for either 1O0H or 1W4O. The highest ligand atom score is 2.4% of the overall CNN score for 1O0H and the two highest scoring atoms for 1W40 are oxygens which appear to be involved

in hydrogen bonding to receptor atoms (66.3% and 50.5%).

OriginalFS (middle). A small contribution to the score can be seen for the terminal phosphate of the ligand in 10OH potentially related to hydrogen bonding to the receptor, although this is not matched by coloring in the receptor. The largest contributions for 1O0H are 1.1% (receptor) and 5.6% (ligand). There are larger ligand contributions for 1W4O (max. 34.5%), but again these are not related to interactions sites on the receptor (max. 1.7%).

TransFS (right). There are stronger signals from atoms in the binding sites of the receptors of both structures. The strongest signals from both the ligand and receptor in 1O0H are for atoms involved in hydrogen bonds between the receptor and terminal ligand phosphate group. The largest contributions are 28.6% (receptor, a nitrogen) and 59.8% (a hydrogen-bonding oxygen on the phosphate group in the ligand). The phosphorous atom in terminal group of the ligand is assigned a score of 35.3%. Similar interactions are picked up for 1W4O, again with atoms involved in hydrogen bonds between the ligand and receptor being highlighted as important to the CNN score. Here, the largest contributions are 38.5% (receptor) and 54.9% (ligand).

These results suggest that training on DUD-E-Trans (TransFS) causes CNNs to score receptor and ligand atoms involved in hydrogen bonding, an effect which has not been shown before. They also suggest that networks trained in this way are learning physical interactions, a requirement for a more generalisable classifier.

Conclusion

In this paper, we have described a method of training data augmentation that improves the generalisability of a deep learning method for structure-based virtual screening. Our

augmentation consists of adding three copies of each active in a random conformation, randomly rotated and translated and labelled as decoys for training. Networks trained with this augmented data also have higher scores associated with receptor and ligand atoms that participate in favourable interactions. Our simple augmentation procedure could be configured for use in many other machine learning methods for ligand binding prediction. The arbitrary choice of using three translated decoys for each active could also be further be tuned, for example using cross-validation on a test set external to the training data.

PDB codes used (PubMed IDs): 1W4O (15670155); 1O0H (14573867)

References

(1) Chen, L.; Cruz, A.; Ramsey, S.; Dickson, C. J.; Duca, J. S.; Hornak, V.; Koes, D. R.; Kurtzman, T. Hidden bias in the DUD-E dataset leads to misleading performance of deep learning in structure-based virtual screening. *PLOS ONE* **2019**, *14*, 1–22.

(2) Sieg, J.; Flachsenberg, F.; Rarey, M. In Need of Bias Control: Evaluating Chemical Data for Machine Learning in Structure-Based Virtual Screening. *Journal of Chemical Information and Modeling* **2019**, *59*, 947–961.

(3) Wallach, I.; Heifets, A. Most Ligand-Based Classification Benchmarks Reward Memorization Rather than Generalization. *Journal of Chemical Information and Modeling* **2018**, *58*, 916–932, PMID: 29698607.

(4) Gimeno, A.; Ojeda-Montes, M.; Tomas-Hernandez, S.; Cereto-Massague, A.; Beltran-Debon, R.; Mulero, M.; Pujadas, G.; Garcia-Vallve, S. The Light and Dark Sides of Virtual Screening: What Is There to Know? *International Journal of Molecular Sciences* **2019**, *20*, 1375.

(5) Lavecchia, A.; Giovanni, C. Virtual Screening Strategies in Drug Discovery: A Critical Review. *Current Medicinal Chemistry* **2013**, *20*, 2839–2860.

(6) Wang, Z.; Sun, H.; Yao, X.; Li, D.; Xu, L.; Li, Y.; Tian, S.; Hou, T. Comprehensive evaluation of ten docking programs on a diverse set of protein–ligand complexes: the prediction accuracy of sampling power and scoring power. *Phys. Chem. Chem. Phys.* **2016**, *18*, 12964–12975.

(7) Carpenter, K. A.; Huang, X. Machine Learning-based Virtual Screening and Its Applications to Alzheimer's Drug Discovery: A Review. *Current Pharmaceutical Design* **2018**, *24*, 3347–3358.

(8) Gonczarek, A.; Tomczak, J. M.; Zareba, S.; Kaczmar, J.; Dabrowski, P.; Walczak, M. J. Interaction prediction in structure-based virtual screening using deep learning. *Computers in Biology and Medicine* **2018**, *100*, 253–258.

(9) Pereira, J. C.; Caffarena, E. R.; dos Santos, C. N. Boosting Docking-Based Virtual Screening with Deep Learning. *Journal of Chemical Information and Modeling* **2016**, *56*, 2495–2506.

(10) Vamathevan, J.; Clark, D.; Czodrowski, P.; Dunham, I.; Ferran, E.; Lee, G.; Li, B.; Madabhushi, A.; Shah, P.; Spitzer, M. e. a. Applications of machine learning in drug discovery and development. *Nature Reviews Drug Discovery* **2019**, *18*, 463–477.

(11) Lee, I.; Keum, J.; Nam, H. DeepConv-DTI: Prediction of drug-target interactions via deep learning with convolution on protein sequences. *PLOS Computational Biology* **2019**, *15*, 1–21.

(12) Altae-Tran, H.; Ramsundar, B.; Pappu, A. S.; Pande, V. Low Data Drug Discovery with One-Shot Learning. *ACS Central Science* **2017**, *3*, 283–293, PMID: 28470045.

(13) Tsubaki, M.; Tomii, K.; Sese, J. Compound–protein interaction prediction with end-to-end learning of neural networks for graphs and sequences. *Bioinformatics* **2018**, *35*, 309–318.

(14) Boyles, F.; Deane, C. M.; Morris, G. Learning from the Ligand: Using Ligand-Based Features to Improve Binding Affinity Prediction. 2019; `https://chemrxiv.org/articles/Learning_from_the_Ligand_Using_Ligand-Based_Features_to_Improve_Binding_Affinity_Prediction/8174525/1`.

(15) Lecun, Y.; Bottou, L.; Bengio, Y.; Haffner, P. Gradient-based learning applied to document recognition. *Proceedings of the IEEE* **1998**, *86*, 2278–2324.

(16) Ragoza, M.; Hochuli, J.; Idrobo, E.; Sunseri, J.; Koes, D. R. Protein–Ligand Scoring with Convolutional Neural Networks. *Journal of Chemical Information and Modeling* **2017**, *57*, 942–957, PMID: 28368587.

(17) Mysinger, M. M.; Carchia, M.; Irwin, J. J.; Shoichet, B. K. Directory of Useful Decoys, Enhanced (DUD-E): Better Ligands and Decoys for Better Benchmarking. *Journal of Medicinal Chemistry* **2012**, *55*, 6582–6594.

(18) Imrie, F.; Bradley, A. R.; van der Schaar, M.; Deane, C. M. Protein Family-Specific Models Using Deep Neural Networks and Transfer Learning Improve Virtual Screening and Highlight the Need for More Data. *Journal of Chemical Information and Modeling* **2018**, *58*, 2319–2330, PMID: 30273487.

(19) Mahmoud, A. H.; Masters, M. R.; Yang, Y.; Lill, M. A. Elucidating the multiple roles of hydration for accurate protein-ligand binding prediction via deep learning. *Communications Chemistry* **2020**, *3*.

(20) Gaulton, A.; Hersey, A.; Nowotka, M.; Bento, A. P.; Chambers, J.; Mendez, D.; Mutowo, P.; Atkinson, F.; Bellis, L. J.; Cibrian-Uhalte, E. e. a. The ChEMBL database in 2017. *Nucleic Acids Research* **2016**, *45*, D945–D954.

(21) Hochuli, J.; Helbling, A.; Skaist, T.; Ragoza, M.; Koes, D. R. Visualizing convolutional neural network protein-ligand scoring. *Journal of Molecular Graphics and Modelling* **2018**, *84*, 96 – 108.

(22) Sundar, V.; Colwell, L. Debiasing Algorithms for Protein Ligand Binding Data do not Improve Generalisation. **2019**,

(23) Trott, O.; Olson, A. J. AutoDock Vina: Improving the speed and accuracy of docking with a new scoring function, efficient optimization, and multithreading. *Journal of Computational Chemistry* **2010**, *31*, 455–461.

(24) Heikamp, K.; Bajorath, J. Large-Scale Similarity Search Profiling of ChEMBL Compound Data Sets. *Journal of Chemical Information and Modeling* **2011**, *51*, 1831–1839.

(25) Sunseri, J.; Koes, D. R. libmolgrid: Graphics Processing Unit Accelerated Molecular Gridding for Deep Learning Applications. *Journal of Chemical Information and Modeling* **2020**,

(26) Berman, H. M. The Protein Data Bank. *Nucleic Acids Research* **2000**, *28*, 235–242.

(27) Saito, T.; Rehmsmeier, M. The Precision-Recall Plot Is More Informative than the ROC Plot When Evaluating Binary Classifiers on Imbalanced Datasets. *PLOS ONE* **2015**, *10*, e0118432.

(28) OpenEye Toolkits. *OpenEye Scientific Software, Santa Fe, NM* **2019**,

Supplementary Material

Protocol 1: Protocol for generation of DUD-E-Trans augmented training set.

First the active ligand molecules are 'moved' into the centre of mass of the protein, then a distance is generated by the following method (R = radius of the protein):

$$
\begin{aligned}
y_1(r) &= \exp\left(-\frac{(r-\mu_1)^2}{2\sigma_1^2}\right) \\
y_2(r) &= \exp\left(-\frac{(r-\mu_2)^2}{2\sigma_2^2}\right) \\
y_3(r) &= \exp\left(-\frac{(r+\mu_2)^2}{2\sigma_2^2}\right) \\
y_4(r) &= 2y_1(r) + y_2(r) + y_3(r) \\
\text{where} \quad \mu_1 &= 0 \quad \sigma_1 = \frac{R}{3.5} \\
\mu_2 &= R \quad \sigma_2 = \frac{R}{2.5}
\end{aligned}
$$

$y_4(r)$ is calculated for a range of 1,000 values of r in the interval $(-1.3R, 1.3R)$. The set of values for $y_4(r)$ is then divided by the total sum of those values, making a discrete distribution over r from which the distance to move the molecule in the direction of a random unit vector is drawn. The OpenEye toolkit[28] is used to randomly rotate and then randomize the conformation of each translated molecule. These new active/target structures are labelled as decoys for training.

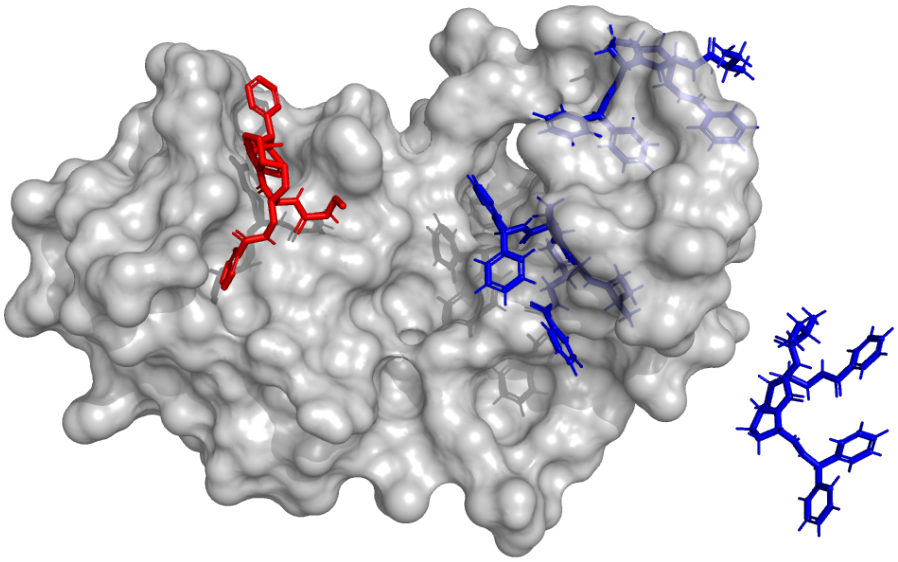

Figure S1: Example of random translations and conformations (shown in blue) of an active molecule (original pose in red) for a protein target (grey), included in the DUD-E-Trans dataset. Blue poses are labelled as decoys in a DUD-E-Trans training set, with red remaining as an active. DUD-E target: XIAP; ligand: CHEMBL584393.

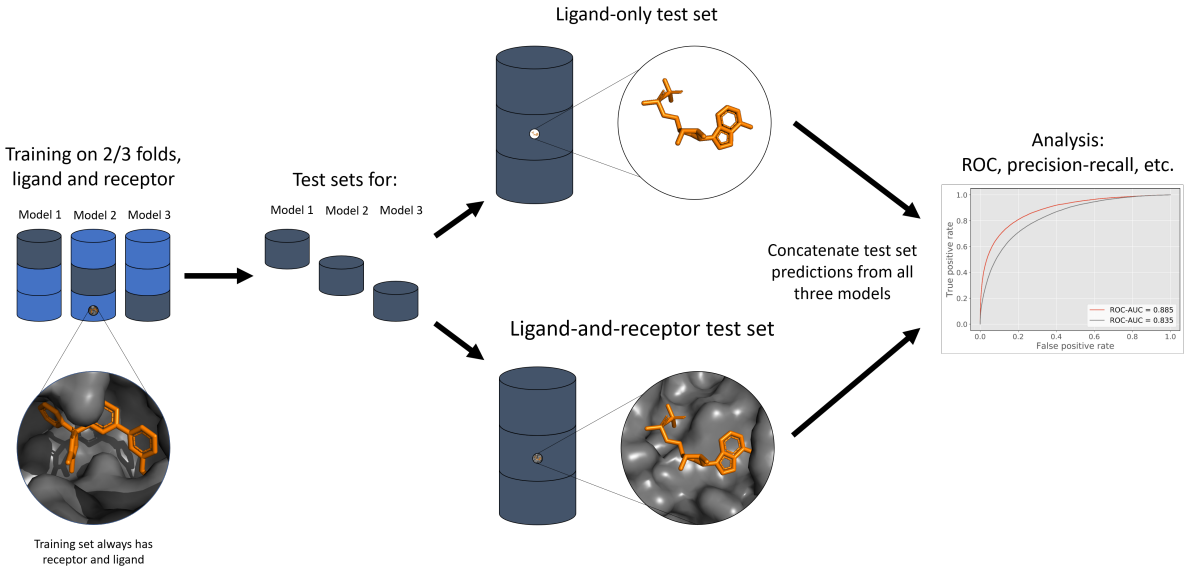

Figure S2: Protocol for training on DUD-E and the Ligand-and-receptor and Ligand-only tests. Three models are trained on 2 folds each (light blue), and tested on both normal and ligand-only versions of the final fold (dark blue). Test predictions from the three models are concatenated for analysis.

Table S1: Target splits for the DUD-E dataset. Targets from different folds have $\leq 80\%$ sequence similarity.

Fold 0		**Fold 1**		**Fold 2**	
Target	Family	Target	Family	Target	Family
abl1	Kinase	akt1	Kinase	csf1r	Kinase
braf	Kinase	akt2	Kinase	kit	Kinase
cdk2	Kinase	egfr	Kinase	mapk2	Kinase
fak1	Kinase	jak2	Kinase	mk14	Kinase
igf1r	Kinase	lck	Kinase	mp2k1	Kinase
kpcb	Kinase	met	Kinase	plk1	Kinase
mk01	Kinase	tgfr1	Kinase	rock1	Kinase
mk10	Kinase	wee1	Kinase	vgfr2	Kinase
src	Kinase	ace	Protease	mmp13	Protease
ada17	Protease	bace1	Protease	lkha4	Protease
casp3	Protease	fa7	Protease	reni	Protease
dpp4	Protease	hivpr	Protease	try1	Protease
tryb1	Protease	fa10	Protease	gcr	Nuclear
urok	Protease	thrb	Protease	mcr	Nuclear
andr	Nuclear	esr1	Nuclear	ppara	Nuclear
ppard	Nuclear	esr2	Nuclear	prgr	Nuclear
drd3	GPCR	pparg	Nuclear	rxra	Nuclear
tysy	Other	thb	Nuclear	aa2ar	GPCR
hdac8	Other	cxcr4	GPCR	adrb1	GPCR
hivrt	Other	aces	Other	adrb2	GPCR
pur2	Other	pyrd	Other	glcm	Other
aofb	Other	pgh1	Other	cah2	Other
inha	Other	parp1	Other	grik1	Other
comt	Other	cp2c9	Other	ital	Other
sahh	Other	def	Other	dhi1	Other
pygm	Other	pnph	Other	fpps	Other
fabp4	Other	pgh2	Other	pde5a	Other
aldr	Other	ada	Other	nos1	Other
fnta	Other	cp3a4	Other	kif11	Other
pa2ga	Other	nram	Other	hivint	Other
xiap	Other	fkb1a	Other	hxk4	Other
hmdh	Other	ptn1	Other	kith	Other
dyr	Other	hdac2	Other	ampc	Other
		gria2	Other	hs90a	Other

	Model 1	Model 2	Model 3	Pose mean
Docked pose 1	0.93	0.91	0.95	0.93
Docked pose 2	0.99	0.90	0.87	0.92
Docked pose 3	0.92	0.94	0.90	0.92
Docked pose 4	0.83	0.85	0.78	0.82
Docked pose 5	0.84	0.71	0.88	0.81
Docked pose 6	0.78	0.77	0.76	0.77
Docked pose 7	0.74	0.72	0.64	0.70
Docked pose 8	0.66	0.66	0.66	0.66
Docked pose 9	0.54	0.60	0.68	0.61

Ligand score
0.88

Figure S3: How a final CNN score is arrived upon given three scores for nine different poses of the same ligand for each target. Each pose is scored by three different models trained in the same way from a different starting configuration; the mean of these three scores is taken, giving nine scores (one per pose), the top five of which are averaged to give the final score.

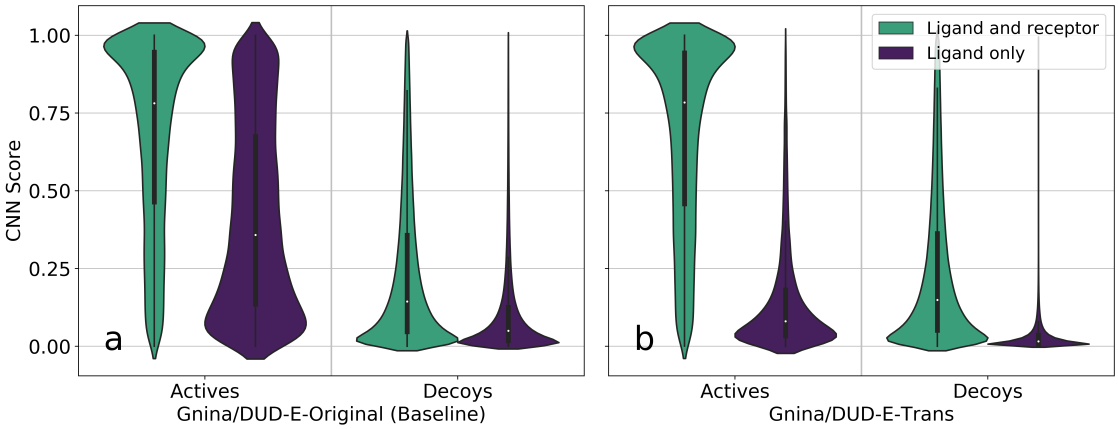

Figure S4: Violin plots of scores given to actives and decoys by Gnina models trained with DUD-E-Original (Baseline) and DUD-E-Trans. Score distributions for test sets with ligand and receptor information present are shown in green; test sets with ligand information only are shown in purple. Plots *a* and *b* show distributions for models trained using DUD-E-Original and DUD-E-Trans respectively.

Table S2: ROC-AUC values for the 14 targets in the ChEMBL validation set for DenseFS models trained either with DUD-E-Original or with the DUD-E-Trans dataset. Highest values in a row are highlighted in bold.

Chembl Target	Family	OriginalFS	TransFS
10752	Kinase	**0.875**	0.854
12670	Kinase	**0.912**	0.910
20014	Kinase	0.934	**0.938**
10378	Protease	0.636	**0.705**
10498	Protease	0.743	**0.769**
11534	Protease	0.804	**0.842**
219	GPCR	0.842	**0.865**
11279	GPCR	0.819	**0.825**
11631	GPCR	**0.845**	0.828
12968	GPCR	0.505	**0.582**
28	Other (Thymidylate synthase)	**0.927**	0.914
276	Other (Phosphodiesterase 4A)	0.868	**0.882**
11359	Other (Phosphodiesterase 4A)	0.834	**0.840**
18061	Other (Sodium channel protein type IX α-subunit)	0.677	**0.693**

Table S3: PR-AUC values for the 14 targets in the ChEMBL validation set for DenseFS models trained with the DUD-E-Original, DUD-E-Trans, DUD-E-Redocked and DUD-E-Hybrid datasets.

Chembl Target	Family	OriginalFS	TransFS	RedockedFS	HybridFS
10752	Kinase	0.289	0.272	0.270	0.272
12670	Kinase	0.363	0.374	0.350	0.335
20014	Kinase	0.573	0.580	0.566	0.525
10378	Protease	0.047	0.052	0.032	0.041
10498	Protease	0.056	0.078	0.073	0.091
11534	Protease	0.062	0.095	0.100	0.103
219	GPCR	0.116	0.153	0.069	0.087
11279	GPCR	0.039	0.039	0.040	0.044
11631	GPCR	0.245	0.264	0.191	0.202
12968	GPCR	0.009	0.011	0.011	0.011
28	Other (Thymidylate synthase)	0.286	0.363	0.297	0.323
276	Other (Phosphodiesterase 4A)	0.318	0.415	0.269	0.375
11359	Other (Phosphodiesterase 4A)	0.214	0.270	0.133	0.195
18061	Other (Sodium channel protein type IX α-subunit)	0.031	0.031	0.032	0.033

Table S4: PRC-AUC values for the 14 targets in the ChEMBL validation set for OriginalFS and DenseFS trained on the entire of their respective training sets, both with and without receptor information available at test time. The right-most column shows results for the TrasnFS models given only ligand information to predict on, and scores are significantly lower than for the corresponding test with OriginalFS.

ChEMBL Target	Family	OriginalFS Ligand and receptor	OriginalFS Ligand only	TransFS Ligand and receptor	TransFS Ligand only
10752	Kinase	0.289	0.300	0.272	0.069
12670	Kinase	0.363	0.348	0.374	0.060
20014	Kinase	0.573	0.548	0.580	0.261
10378	Protease	0.047	0.059	0.052	0.089
10498	Protease	0.056	0.059	0.078	0.076
11534	Protease	0.062	0.062	0.095	0.058
219	GPCR	0.116	0.078	0.153	0.123
11279	GPCR	0.039	0.032	0.039	0.016
11631	GPCR	0.245	0.213	0.264	0.095
12968	GPCR	0.009	0.009	0.011	0.009
28	Other	0.286	0.295	0.363	0.193
276	Other	0.318	0.272	0.415	0.054
11359	Other	0.214	0.162	0.270	0.031
18061	Other	0.031	0.029	0.031	0.012

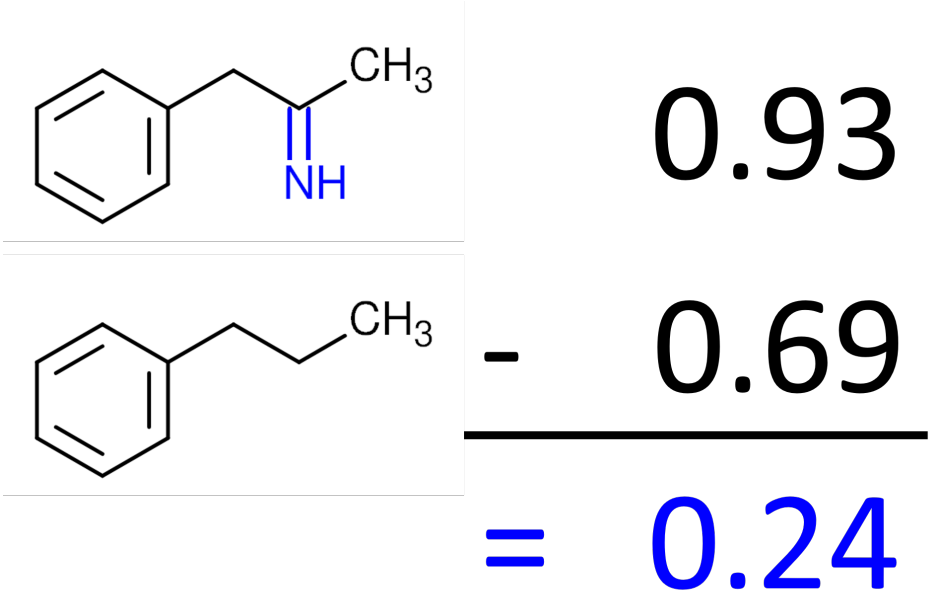

Figure S5: Atomistic masking. The contribution of each atom is given by the difference in scores when the atom is present compared to when it is not.
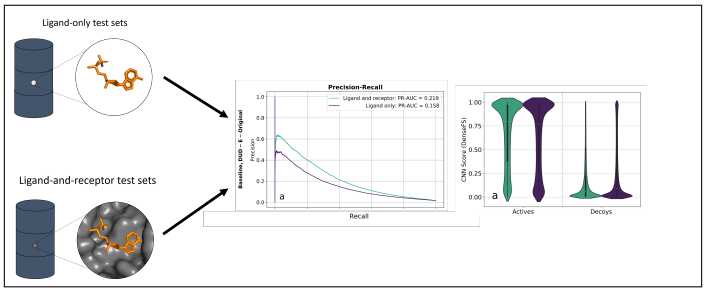
Graphical TOC Entry